CSIRO PUBLISHING

International Journal of Wildland Fire **2017**, *26*, 685–692
https://doi.org/10.1071/WF17035

Downdraft outflows: climatological potential to influence fire behaviour

Brian E. Potter[A,C] *and Jaime R. Hernandez*[B]

[A]USDA Forest Service, Pacific Northwest Wildfire Laboratory, 400 N 34th Street, Suite 201, Seattle, WA 98103, USA.
[B]College of Idaho, 2112 Cleveland Boulevard, Caldwell, ID 83605, USA.
[C]Corresponding author. Email: bpotter@fs.fed.us

Abstract. Sudden wind shifts caused by atmospheric gust fronts can lead to firefighter entrapments and fatalities. In this study, we describe the physical processes involved in the related phenomena of convective downdrafts, gust fronts and downbursts. We focus on the dominant process, evaporative cooling in a dry surface layer, as characterised by the measure known as downdraft maximum available potential energy (DMAPE). We present a climatological analysis of DMAPE for the coterminous United States, developed from the Climate Forecast System Reanalysis data for the period 1979–2008. Diurnal and seasonal patterns are described. We conclude with a discussion of the implications and limitations of the analysis and DMAPE as an indicator of gust front strength or downburst occurrence.

Additional keywords: DMAPE, downburst, downdraft maximum available potential energy, wind shift.

Received 14 February 2017, accepted 19 May 2017, published online 8 August 2017

Introduction

A change in wind direction, a wind shift, is one of the greatest dangers to wildland firefighters. It turns a flank to a head, pushing it into areas previously considered safer and lower-intensity. Several different phenomena can produce a wind shift. Terrain can channel otherwise small wind shifts, producing more abrupt shifts and increases in speed. In some areas, terrain interacts with local diurnal effects like land–sea breezes or slope flows, to produce wind shifts. Frontal passages (including the often-cited breakdown of an upper level ridge), thermal troughs and dry lines can cause wind shifts as well. All of these shifts are currently predictable hours or more in advance – they are either recurring phenomena at a location, or they are large-scale events that weather prediction models capture well.

The most dangerous wind shifts for firefighters are sudden changes in wind direction, with an increase in wind speed. Thunderstorms produce a wind shift known as a gust front or outflow boundary. Gust fronts range from persistent boundaries flowing out ahead of a long-lived thunderstorm, to downbursts – surges lasting tens of minutes and only travelling a few kilometres. Gust fronts can remain long after the storm producing them has dissipated, and can travel tens of kilometres. The Ransom Road Fire Report (Surveys and Investigation Staff 1981), Goens and Andrews (1998), the 2004 Saint Sebastian Prescribed Fire Burnover Report (Kern *et al.* 2004), Yarnell Hill Fire Serious Accident Investigation Report (Karels *et al.* 2013) and Johnson *et al.* (2014) all cited gust fronts as the cause of the entrapments of wildland fire fighters, deaths or destruction of homes. Haines (1988) described the general dangers of downbursts on wildland fires, using Ransom Road as his example. (The Ransom Road Report also references a fire fatality due to a gust front in Okefenokee Wildlife Refuge, in 1979.) In some cases, these were long-lived gust fronts; in others, they were the result of short-lived downbursts.

Given the safety implications of downbursts, there is value in having information on their potential occurrence. In this paper, we briefly describe the basic processes that influence thunderstorm outflow boundaries. We describe a measure, downdraft maximum available potential energy (DMAPE), of one of those processes, including its limitations. We then present a climatological analysis of the diurnal and seasonal variations of DMAPE. We conclude with a discussion of the implications and limitations of the analysis, with respect to the science and management of wildland fire.

Downdraft dynamics

Detailed discussions of storm dynamics, including downdrafts, can be found in Houze (1993, pp. 319–327), Wakimoto (1985), Srivastava (1985, 1987), Mueller and Carbone (1987), Knupp (1987), Atkins and Wakimoto (1991) and Gilmore and Wicker (1998). Wakimoto (1985) most directly considers downbursts, whereas Mueller and Carbone (1987) go into the most detail about overall thunderstorm dynamics. Thunderstorm circulations include more than one type of downdraft, and it is the evaporation-driven downdraft that is largely responsible for the gust front and related wind shifts. The present discussion considers only that downdraft and related processes.

When a convective cell rises upward in the atmosphere, condensation and freezing lead to the formation of water droplets and ice crystals. Some of these may grow large enough to fall out of the convective updraft, heading back towards the ground. Variations in wind speed and direction with height mean the convective updraft is not purely vertical, and the precipitation will fall outside the updraft into environmental air. As that precipitation falls into unsaturated air, ice melts and water evaporates, cooling the air. This cooling increases the air's density, creating a negative buoyant force and moving the air downward. Simultaneously, the frictional drag of the precipitation pulls air with it, reinforcing the negative buoyancy. As long as precipitation continues to fall through the air and the air remains unsaturated, the cooling continues, maintaining or increasing the magnitude of the negative buoyant force. Drag also persists as long as there is precipitation. Entrainment of environmental air during descent may modify the rate of evaporation, as well as the air's density and rate of descent, depending on the temperature, humidity and density of the entrained air. When the descending air reaches the ground, it spreads out laterally. Initial horizontal momentum may influence that spread, pushing the air in a particular direction. The descending air is the evaporative downdraft, and the horizontal spread of the air constitutes the storm outflow, or if it is particularly intense, may be strong enough to be classified as a downburst.

Kessinger *et al.* (1988) estimated that drag produces ~20% of the downward acceleration, based on radar observations of precipitation in a downburst and the vertical momentum equation. Following their approach and using precipitation and temperature values from Proctor's (1989) numerical modelling study of downdrafts yields a drag contribution range of 0.3 to 66%, with higher values for higher precipitation amounts. In dry environments, it is unlikely the water mass would reach Proctor's upper limit, but it is not unheard of in wetter environments. Accounts of downbursts on wildland fires often mention the sudden temperature drop as the wind shift occurs. Without evaporative cooling, the descending air would warm due to adiabatic compression, so any time there is cooling, it must be a result of the evaporative contribution, not the precipitation drag.

Wakimoto (1985) differentiated between 'wet' and 'dry' downbursts based on whether or not precipitation accompanied the strong winds at the ground. The former are more common in humid areas, like the south-east, whereas the latter are more common in regions such as the west slope of the Rocky Mountains and the desert south-west of the United States. Wakimoto (1985) and Atkins and Wakimoto (1991) examined temperature and moisture profiles from field experiments and determined that both wet and dry downbursts typically had an 'inverted V' appearance on skew *T*–log *p* diagrams (*T* indicating temperature, *p* indicating pressure), as shown in Fig. 1. The depth of the 'V' was close to 500 hPa for dry downburst soundings, but as shallow as 100 hPa for wet downburst soundings. (The shallower 'V' for wet downbursts is also consistent with the above calculations from Proctor (1989) in supporting the role of drag in these types of downbursts.)

The vertical wind profile is a critical factor in this whole process. The directional and speed profiles of the wind can make the difference between a small, short-lived convective system and a sustaining storm system that propagates for tens or hundreds of kilometres. The wind profile also determines where any downdrafts will be strongest. Although studies have looked at wind profiles' importance in storm dynamics (e.g. Knupp 1987; Gilmore and Wicker 1998), there is no single clear or simple profile associated with strong downdrafts or downbursts. For the present discussion, what matters is that the precipitation falls into a deep, dry layer of air somewhere lateral to the convective updraft. This maximises the potential evaporation of the precipitation, and the potential speed of the downdraft, all other factors being equal. When the downdraft strikes the ground, it will spread horizontally, creating a gust front that brings the sudden wind shift and increased wind speed of concern to firefighters.

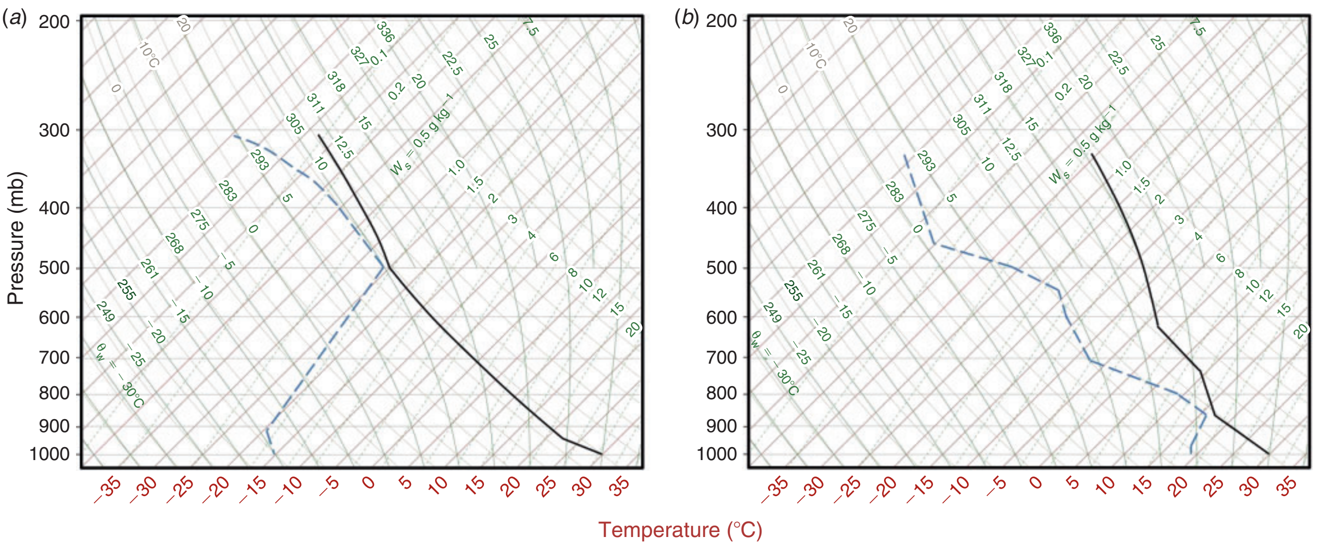

Fig. 1. Idealised skew *T*–log *p* (*T*, temperature; *p*, pressure) soundings for (*a*) dry downbursts, and (*b*) wet downbursts. Black lines indicate temperature profiles, dashed blue lines indicate dew-point profiles. The dry profile is based on Wakimoto (1985), the wet profile is based on Atkins and Wakimoto (1991).

The downburst event during the Dude Fire is sometimes described as a product of the fire's own convection, at other times as the product of a nearby thunderstorm. Anecdotes in the field occasionally mention downbursts from fire convective plumes. Given observations of hail or rain from some fire plumes, it is possible that some fires generate their own evaporatively driven downdrafts and gust fronts. The present study does not consider or depend on whether an outflow develops due to pyroconvection, or non-fire convection. The force lifting the updraft is irrelevant to the environmental potential for a downdraft-driven gust front.

DMAPE

One measure of the potential energy of a downdraft when it reaches the ground is downdraft maximum available potential energy (DMAPE). DMAPE quantifies the evaporative potential of the atmosphere. It does not incorporate any consideration of the wind profile, nor does it include any determination of how much precipitation is available to evaporate, nor how entrainment during descent might modify the potential downdraft. It is commonly known as downdraft convective available potential energy (DCAPE) in the United States, but because of the aforementioned assumptions and limitations, DMAPE (the Australian name) is more accurate. Gilmore and Wicker (1998) used a numerical atmospheric model to simulate downdrafts and downbursts, finding that entrainment during descent and limited evaporation of rain prevent DMAPE from fully realising. Because of these and other possible factors, as little as 10% of DMAPE actually manifested in some cases. This point is considered further in the *Discussion* section.

DMAPE measures the energy available from the negative buoyancy of a parcel of air as it descends from a given starting height to the ground, continuously saturated by evaporating precipitation. Because it does not include any entrainment, it does not depend on atmospheric moisture at any level other than the starting level. It does not include sublimation or melting of solid-phase precipitation. It assumes precipitation adequate for continuous saturation as the air descends.

The equation to calculate DMAPE for a parcel of air is (Gilmore and Wicker 1998):

$$\mathrm{DMAPE} = g \int_{z_{sfc}}^{z_0} \frac{\bar{\theta}(z) - \theta(z)}{\bar{\theta}(z)} dz \qquad (1)$$

Here, g is the acceleration due to gravity (m s^{-2}); z_0 is the height at which the air starts its descent (m); z_{sfc} is the height of the ground (m) where descent ends; $\bar{\theta}(z)$ is the environmental potential temperature (K) as a function of height; and $\theta(Z)$ is the descending parcel's potential temperature (K) as a function of height. The choice of z_0 is discussed below in the *Methods* section.

Fig. 2 shows DMAPE as the area below z_0 and between the saturated adiabat of the descending parcel and the environmental

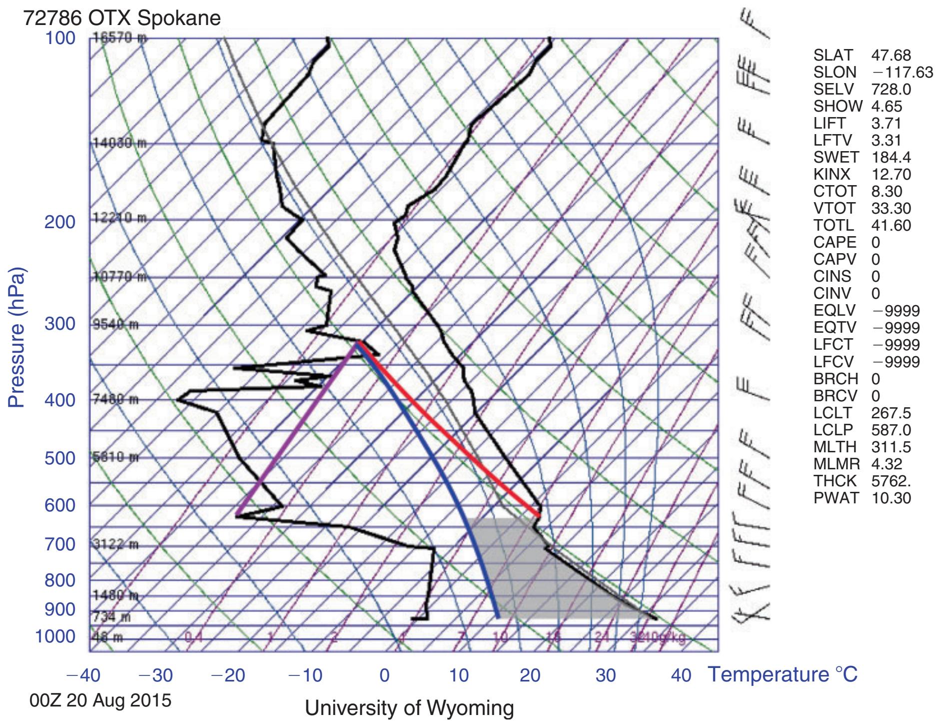

Fig. 2. Graphic illustration of downdraft maximum available potential energy (DMAPE). This example using the observed sounding for Spokane, WA, at 0000 UTC on 20 August 2015 shows DMAPE for air starting at a height of 4032 m (626 hPa). The red line indicates the dry adiabat of the air at this level, whereas the purple line indicates constant mixing ratio for that air. The blue curve between them is the moist adiabat of the air as it descends with constant saturation. The shaded area represents the relative value of DMAPE; see text for details.

temperature profile on a skew T–log p diagram. The appropriate saturated adiabat can be determined graphically by following the dry adiabat of air at the starting height, z_0, upwards to the lifted condensation level, then lowering it along the saturated adiabat from that level. A higher starting height, a wider separation of the saturated adiabat from the environmental profile, or a combination of these two factors will result in a higher value of DMAPE. Because DMAPE does not include any precipitation drag component, it is an incomplete metric for wet downbursts.

Data and methods

We used the National Oceanic and Atmospheric Administration National Center for Environmental Prediction's (NOAA NCEP) Climate Forecast System Reanalysis (CFSR, Saha *et al.* 2010) data for the 30-year period 1979 to 2008. This dataset contains temperature and moisture (relative humidity) data at standard atmospheric pressure levels. DMAPE was computed for 0000, 0600, 1200, and 1800 UTC (Coordinated Universal Time) each day over the period of study.

There are several precedents for how one selects the starting height, z_0, for the DMAPE computation. Gilmore and Wicker (1998) refer to 'the level of minimum θ_w at midlevels', where θ_w is wetbulb potential temperature (K), but do not specify what constitutes 'midlevels'. Rasmussen and Blanchard (1998) used the highest DMAPE resulting from several levels spaced 1 km vertically, starting 1 km above ground (they do not specify a maximum starting height). Craven and Brooks (2004) chose the level of minimum θ_w between 700 and 500 hPa. Naylor *et al.* (2012) used a method similar to Rasmussen and Blanchard (1998), but only considered starting heights of 3, 4 or 5 km above ground level. The Storm Prediction Center daily Sounding Analysis website uses the level of minimum θ_w in the lowest 400 hPa (http://www.spc.noaa.gov/exper/soundings/help/params2.html, accessed 2 May 2017).

For the present study, the starting height for DMAPE calculations followed the Storm Prediction Center's approach, taking z_0 as the level of minimum wet-bulb potential temperature (θ_w) in a ground-based 400-hPa-deep layer. That θ_w level is the same as the level of minimum equivalent potential temperature (θ_e), however, and the latter is much easier to compute. Thus, we used the level of minimum equivalent potential temperature (hereafter $L_{min}\theta_e$) as our starting height for descending air.

Values of DMAPE were computed using C++ code written for this study. Computations used GNU science library statistical functions (Galassi *et al.* 2009). Statistics computed included monthly and seasonal values of the average, standard deviation, 50th, 75th, 90th and 95th percentiles for both DMAPE and $L_{min}\theta_e$ for each of the four daily times available. Seasons were defined as winter (December, January and February), spring (March, April and May), summer (June, July and August) and fall (autumn) (September, October and November).

Results

Diurnal cycle

To illustrate the diurnal cycle in DMAPE, we plotted the 6-hourly values at four locations (Table 1), for each season. The locations were chosen based on visual inspection of the 6-hourly seasonal maps to show diurnal variations observed in the CFSR data. Fig. 3 shows the diurnal cycles for these locations and the four seasons. For all seasons, the eastern locations peak at 1800 UTC, whereas the western locations reach peak DMAPE later in the day, at 0000 UTC. Overall, the western diurnal cycle has a larger amplitude than the eastern diurnal cycle in all seasons. Winter values are so low that there is little amplitude in the diurnal cycle. At northerly latitudes, spring and autumn values and diurnal patterns are similar. The summer diurnal cycle for Syracuse shows values increasing from 0600 to 1200 UTC, which is 0200 to 0800 Eastern Daylight Time (EDT). The early sunlight at high latitudes is evidently sufficient to start heating the surface layers of the atmosphere and generating DMAPE. In the south-west, DMAPE drops more strongly at night (0600 to 1200 UTC) in summer than any other season, or any other location between these times.

Table 1. Locations used to examine the diurnal cycle in downdraft maximum available potential energy (DMAPE)

Location name	Latitude	Longitude
Syracuse, New York	43°03′N	76°09′W
Columbus, Georgia	32°30′N	85°00′W
Yuma, Arizona	32°40′N	114°36′W
Boise, Idaho	43°37′N	116°16′W

Examination of $L_{min}\theta_e$ (not shown) reveals diurnal patterns of similar nature, suggesting the diurnal signal in DMAPE arises from two components. First, the environmental profile warms during the day, moving the right side of the shaded area in Fig. 2 further right. Second, at the same time that the boundary layer warms, $L_{min}\theta_e$ moves upward and the shaded area expands at the top.

Annual cycle

For brevity, this discussion focuses on the seasonal maps. Specific months are cited when they clarify the seasonal patterns. Emphasis is also on 0000 UTC mean values, with some discussion of 1800 UTC values.

During winter (Fig. 4*a*), mean DMAPE is less than 200 J kg^{-1} over all of the United States except for Florida, where it is between 200 and 400 J kg^{-1}. Values are larger across the country in spring (Fig. 4*b*), with greatest values in the south. The northern Rocky Mountains, the Pacific Northwest west of the Cascade Mountains, and the area north-east of a line running approximately from the Montana–North Dakota–Canada intersection to the southern tip of Maryland show average DMAPE below 200 J kg^{-1}. The highest mean values in spring appear over the lower Rio Grande River and the Sonoran Desert, between 600 and 800 J kg^{-1}.

The same general spatial patterns appear in summer (Fig. 4*c*). The Sonoran Desert region has mean values above 1000 J kg^{-1}, still the highest across the country. An area with mean DMAPE greater than 800 J kg^{-1} extends from the southern tip of Nevada down to the United States–Mexico border, to Texas' coast and from there north into the southern Great Plains. Much of the rest of the US has mean DMAPE values between 600 and 800 J kg^{-1}, with exceptions at higher elevations, along the coasts, and in the

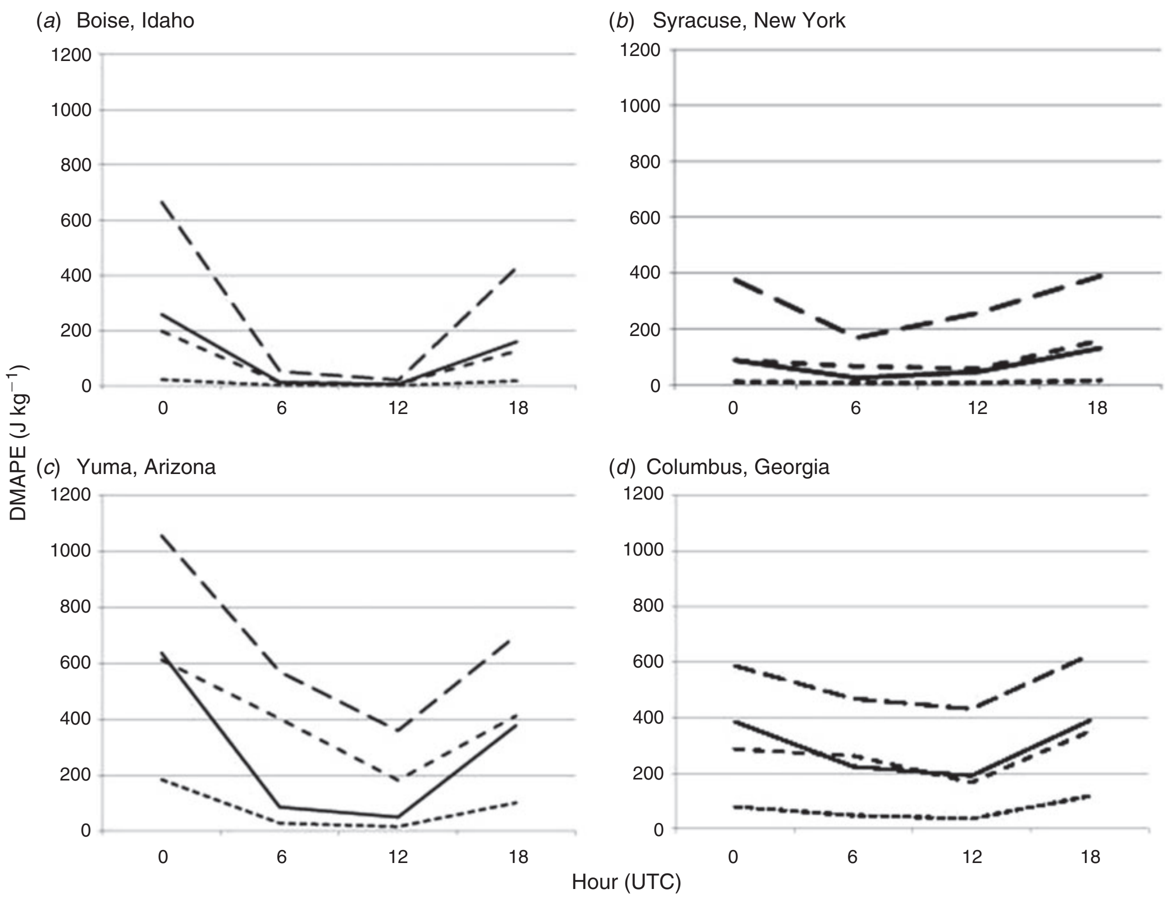

Fig. 3. Diurnal cycles in downdraft maximum available potential energy (DMAPE) for four reference locations, by season. Solid lines indicate spring values, long dashes indicate summer values, medium dashes are autumn values and short dashes are winter values.

same area of the north-east where values were low in spring. Within the summer months of June, July and August, the southern Great Plains reach their maximum mean values during July, whereas the Sonoran Desert does so in August. More generally, July appears to bring maximum mean values east of the Rocky Mountains, and August to the west side of the Rockies.

Autumn mean values (Fig. 4*d*) are lower than summer, and lower than spring as well. The one exception to this spring *v*. autumn comparison is along the Gulf of California, where the region with DMAPE between 600 and 800 J kg^{-1} is approximately the same in autumn and spring.

Seasonal patterns at 1800 UTC are similar. Values across most of the United States are lower at 1800 UTC than at 0000 UTC, except in the north-eastern states. There, earlier sunrise produces higher values at 1800 UTC than at 0000 UTC during all seasons except winter (when 1800 and 0000 UTC DMAPE maps are almost indistinguishable). In the summer, longer daylight at high latitudes also contributes to high mean DMAPE values for the north-east.

The arid south-western United States is a logical region for high DMAPE values, but why values would be greatest in the Sonoran Desert specifically is not immediately apparent. Literature on summertime synoptic conditions of the Sonoran Desert (e.g. Badan-Dangon *et al.* 1991; Bordoni and Stevens 2006) suggests that surface heating produces a deep mixed layer, increasing the difference in the numerator of Eqn 1. Summertime convection in the region tends to focus over the Mogollon Rim, to the north-east, concentrating any moisture there and potentially producing subsidence over the rest of the Sonoran Desert. This is conjecture at present, and a subject where future research could be highly insightful.

Discussion

These maps provide a crucial piece of the picture of downburst potential, but they are only one piece. As noted earlier, DMAPE does not incorporate several factors that determine how much of this potential energy manifests. Precipitation must be available and must fall into clear air to evaporate. That evaporation must be sufficient to keep the downdraft saturated. Precipitation drag, which is important for wet downbursts, is not part of the calculation model. The wind profile must favour both convective cell growth (to produce the precipitation) and the precipitation falling into the clear air. The wind profile needed to sustain or support convective growth is well studied (see Houze 1993) but present understanding of downdrafts does not identify optimal wind profiles for downdraft development, and models do not

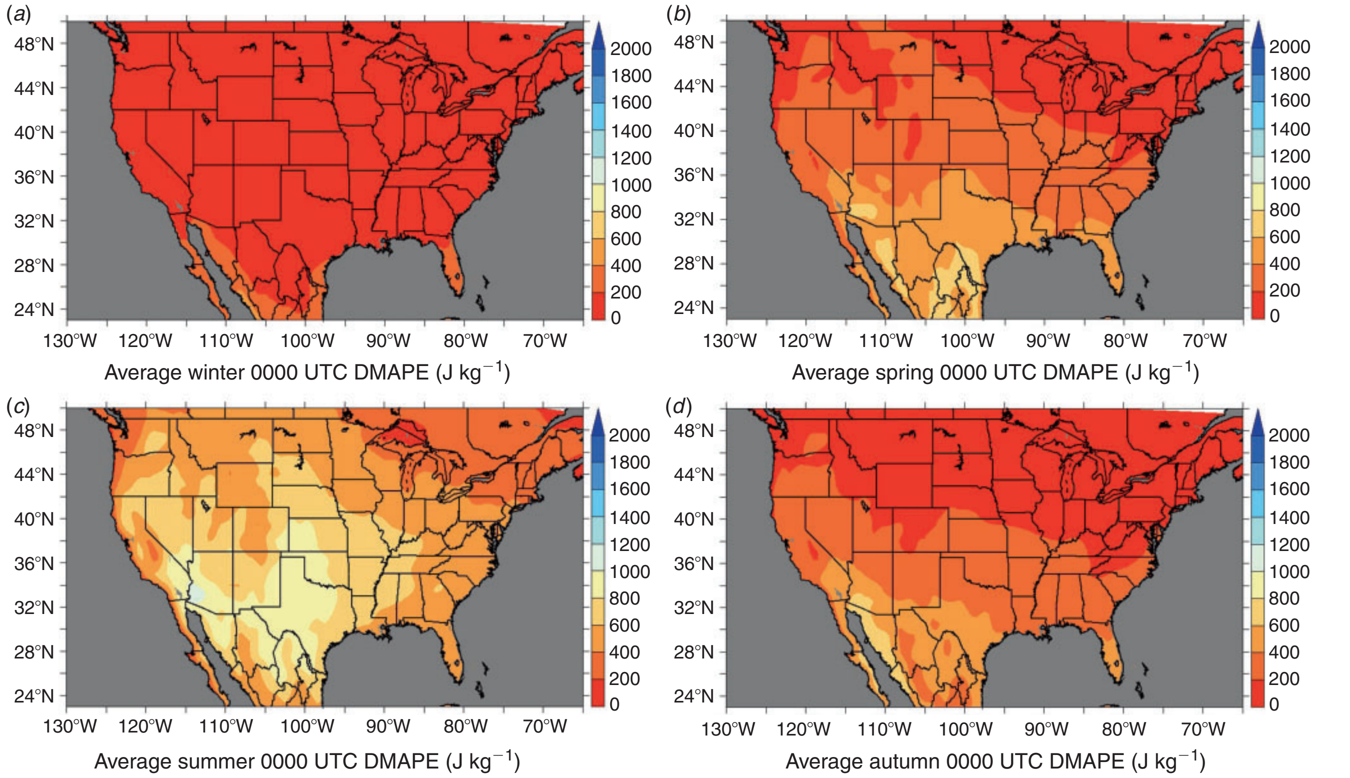

Fig. 4. Average downdraft maximum available potential energy (DMAPE) for (*a*) winter; (*b*) spring; (*c*) summer; (*d*) autumn. Values are in joules per kilogram.

allow timely prediction of the other factors. Imperfect as DMAPE may be, Kuchera and Parker (2006) found it was the best of a suite of thermodynamic variables they tested in their efforts to develop a parameter to predict the potential for damaging winds.

The earlier computations considering precipitation drag's contribution to downdraft momentum, and the characteristic profile for wet downbursts from Atkins and Wakimoto (1991) reproduced in Fig. 1*b* illustrate why DMAPE should not be used to assess the potential for wet downbursts. These downbursts acquire a larger portion of their energy from precipitation drag. They appear to originate from lower levels, as low as 100 hPa above the surface as opposed to as high as 400 hPa using the height-cap imposed by the Storm Prediction Center methodology we adopted. In geometric height, that translates to a difference between ~1000-m height for wet downbursts, and 4200 m for dry downbursts. For wet downbursts, DMAPE can be expected to underestimate the energy of a downburst, a significant difference from its interpretation for dry downbursts.

Revisiting the fires noted in the introduction provides a sense of the climatology's possible use. We extracted DMAPE from the CFSR for each of the fires' relevant individual days, using the grid cell that contained the fires' locations. Table 2 lists the fires, with the CFSR values of DMAPE from 0000 UTC and 1800 hours UTC the day of the fire event, as well as the average, 50th, 75th, 90th and 95th percentile DMAPE values for that location. For the two western fires, DMAPE at 1800 UTC on the day of the wind shifts was at or above the 95th percentile. For the Waldo Canyon Fire, the 0000 UTC value was also near the 95th percentile, but for the Dude Fire, the 0000 UTC value is below 50th percentile. (The Yarnell Hill fire cannot be examined in the same way, because it occurred in 2013 and the CFSR record ends in 2012.)

Table 2. Downdraft maximum available potential energy (DMAPE) values (J kg^{-1}) on the days of known fire-downburst events cited in the Introduction

Percentile values for the locations and months of the events are also shown. UTC, Coordinated Universal Time

Fire	Time	DMAPE	Average	50th	75th	90th	95th
Dude Fire	1800 UTC	1332	645	646	915	1133	1241
	0000 UTC	733	778	819	1061	1247	1332
Waldo Canyon	1800 UTC	1072	575	590	820	984	1074
	0000 UTC	1042	451	397	663	922	1050
Ransom Road	1800 UTC	694	535	529	694	828	919
Saint Sebastian	1800 UTC	355	335	324	447	568	633
Okefenokee NWR	1800 UTC	400	227	219	334	455	522

The three eastern (Florida) fires varied more in terms of how DMAPE at the time of the event compares with the climatological values. (Only 1800 UTC values are considered here, as 0000 UTC is well after the time of the events.) The Saint Sebastian Fire DMAPE was between 50th and 75th percentile, whereas Ransom Road's DMAPE was equal to the 75th percentile. Okefenokee NWR's DMAPE was between the 75th and 90th percentiles for

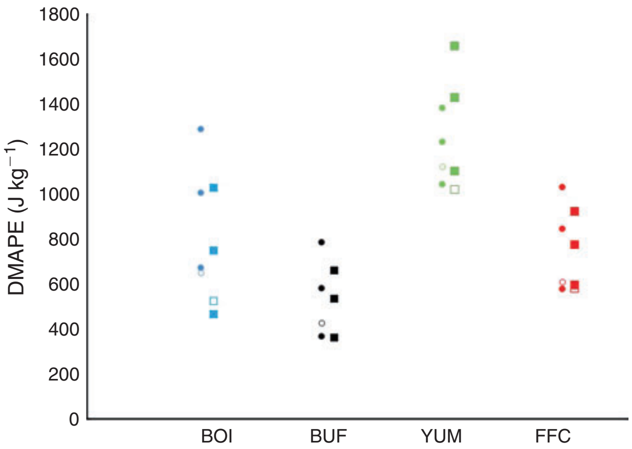

Fig. 5. Comparison of Climate Forecast System Reanalysis (CFSR)-derived downdraft maximum available potential energy (DMAPE) values (squares) and Storm Prediction Center observationally based DMAPE values (circles). Open symbols show mean values, filled symbols indicate 50th, 75th and 90th percentile values from bottom to top respectively. Locations are Boise, Idaho (BOI); Buffalo, New York (BUF); Yuma, Arizona (YUM); Atlanta, Georgia (FFC).

its location and month. All of these were likely wet downbursts, however, and DMAPE being climatologically low during these events may not mean very much.

We noted earlier that Gilmore and Wicker (1998) found as little as 10% of calculated DMAPE actually manifested as air sank to the ground. For any amount of DMAPE that does manifest as the air sinks, an even smaller amount will be present in horizontal outflow winds, because some will be lost in the turbulent process of the air turning from a vertical to a horizontal current. It is unlikely that anything near 100% of calculated DMAPE would ever translate to horizontal wind. Even 10% can be enough to dangerously increase fire intensity and spread rate. Wind speed produced by a given amount of potential energy is equal to the square root of that potential energy. For Waldo Canyon, as an example, 10% of the 0000 UTC DMAPE (Table 2) would be 104 J kg^{-1}, converting to 10 m s^{-1} – more than enough to produce dangerous changes in fire intensity, and possibly reverse the direction of spread or double the rate of that spread.

The climatology's diurnal results also provide some guidance for operational forecasting. Forecasts that present widely different timing for maxima or minima can be identified and given further scrutiny. Individuals without access to more detailed numerical predictions can extrapolate conditions through the day, based at least on climatological norms.

Every numerical atmospheric model and every reanalysis has parameterisations and biases that will affect DMAPE computed from its temperature and humidity profiles, at any location and time. No two models or reanalyses will yield the same value of DMAPE for a given location and time, even if the models or reanalyses are initialised with the same data. No model or reanalysis will match observations after initialisation, either. Fig. 5 illustrates this point. It shows percentile and mean DMAPE values for four locations, for both the CFSR reanalysis data used here and the Storm Prediction Center's observation-based DMAPE climatology. Periods of analysis differ, but the graph still demonstrates how the percentile values differ in the two source datasets, and that the nature of those differences varies across the four locations. The results for Yuma, Arizona, suggest the need for some investigation into why the two datasets differ so much in that area.

We used CFSR for the present study because it is one of the newer reanalyses and it is available for an extended historical period. Because of the aforementioned differences and sensitivities, any direct comparison of the present study's results with observations or daily weather forecasts requires caution and consideration of model or reanalysis differences.

Interpretation of DMAPE for fire purposes requires consideration of at least two other factors. First, to be a fire risk, there must be a chance of fire, meaning available fuels. Second, there must be a chance of convective development to precede any possible downburst. Future work juxtaposing available fuel maps, DMAPE maps, and convective available potential energy (CAPE) maps may yield insight into the interplay among these factors.

Summary

Spatial and seasonal patterns of DMAPE depend on several properties of the atmospheric profile. The presence of dry air in the middle troposphere, the magnitude of the dryness *in situ*, the height of the dry air and the density of that air descending saturated relative to the ambient air density all combine to determine DMAPE. This climatological analysis reveals some information on how those properties interact across the landscape. It also shows variations in the diurnal and seasonal DMAPE cycles across the United States.

DMAPE is only one way of quantifying part of the environment important for downburst formation, and it is less suited to wet downburst situations than it is to dry downbursts. Other elements, as noted in the introduction, include sufficient low-level moisture to allow formation of precipitation, and wind shear conducive to both storm development and precipitation falling into clear air. Operational forecasters need to synthesise all of these potential contributions to determine downburst potential for any specific situation.

Conflicts of interest

The authors declare no conflicts of interest.

Acknowledgements

The authors thank Chuck Maxwell of the National Interagency Fire Center's (NIFC) Southwest Coordination Center and Tom Rolinski of the NIFC Southern California Coordination Center for their conversations about climate of the Sonoran Desert region. Dr Jay Charney with the USDA Forest Service in Lansing, Michigan, also provided many helpful suggestions. Mr Hernandez worked on this project as an intern in the Hispanic National Intern Program, part of the Hispanic Association of Colleges and Universities. The work was financially supported by the USDA Forest Service Pacific Northwest Research Station's National Fire Plan.

References

Atkins NT, Wakimoto RM (1991) Wet microburst activity over the south-eastern United States: implications for forecasting. *Weather and Forecasting* **6**, 470–482. doi:10.1175/1520-0434(1991)006<0470:WMAOTS>2.0.CO;2

Badan-Dangon A, Dorman CE, Merrifield MA, Winant CD (1991) The lower atmosphere over the Gulf of California. *Journal of Geophysical Research* **96**, 16877–16896. doi:10.1029/91JC01433

Bordoni S, Stevens B (2006) Principal component analysis of the summertime winds over the Gulf of California: a gulf surge index. *Monthly Weather Review* **134**, 3395–3414. doi:10.1175/MWR3253.1

Craven JP, Brooks HE (2004) Baseline climatology of sounding-derived parameter associated with deep moist convection. *National Weather Digest* **28**, 13–24.

Galassi M, Davies J, Theiler J, Gough B, Jungman G, Alken P, Booth M, Rossi F (2009) 'GNU Scientific Library Reference Manual'. 3rd edn (for version 1.12). (Network Theory Ltd., UK)

Gilmore MS, Wicker LJ (1998) The influence of mid-tropospheric dryness on supercell morphology and evolution. *Monthly Weather Review* **126**, 943–958. doi:10.1175/1520-0493(1998)126<0943:TIOMDO>2.0.CO;2

Goens DW, Andrews PL (1998) Weather and fire behavior factors related to the 1990 Dude Fire near Payson, Arizona. In 'Proceedings, 2nd Conference on Fire and Forest Meteorology', 11–16 January 1998, Phoenix, AZ, USA. pp. 153–158. (American Meteorological Society, Boston, Massachusetts).

Haines DA (1988) Downbursts and wildland fires: a dangerous combination. *Fire Management Today* **49**, 8–10.

Houze RA, Jr (1993) 'Cloud dynamics.' (Academic Press, San Diego, CA, USA).

Johnson RH, Schumacher RS, Ruppert JH, Jr, Lindsey DT, Ruthford JE, Kriederman L (2014) The role of convective outflow in the Waldo Canyon Fire. *Monthly Weather Review* **142**, 3061–3080. doi:10.1175/MWR-D-13-00361.1

Karels J, Dudley M, Apuzzo G, Carbone L, Draeger R, Foley T, Gonzales R, Kurth J, Manwaring R, Mayhew B, Okon R, Petrilli T, Phipps J, Rocha J, Wachter JB, Wilson R, Ziegler J, Zimmerman T (2013) Yarnell Hill Fire June 30, 2013 Serious Accident Investigation Report. 23 September 2013, Phoenix, AZ, USA. Available at http://www.iawfonline.org/Yarnell_Hill_Fire_report.pdf [Verified 3 June 2016]

Kern J, Jones W, Murrian J, DiMaggio J (2004) Review of burnover incident at St Sebastian River Preserve State Park, Indian River County, Florida, 24 February 2004. April 2004. Available at http://www.wildfirelessons.net/HigherLogic/System/DownloadDocumentFile.ashx?DocumentFileKey=83ebf8a1-1d12-001c-32b5-d279c795fa6b&forceDialog=1 [Verified 6 June 2017].

Kessinger CJ, Parsons DB, Wilson JW (1988) Observations of a storm containing mesocyclones, downbursts, and horizontal vortex circulations. *Monthly Weather Review* **116**, 1959–1982. doi:10.1175/1520-0493(1988)116<1959:OOASCM>2.0.CO;2

Knupp KR (1987) Downdrafts within High Plains cumulonimbi. Part I: General kinematic structure. *Journal of the Atmospheric Sciences* **44**, 987–1008. doi:10.1175/1520-0469(1987)044<0987:DWHPCP>2.0.CO;2

Kuchera EL, Parker MD (2006) Severe convective wind environments. *Weather and Forecasting* **21**, 595–612. doi:10.1175/WAF931.1

Mueller CK, Carbone RE (1987) Dynamics of a thunderstorm outflow. *Journal of the Atmospheric Sciences* **44**, 1879–1898. doi:10.1175/1520-0469(1987)044<1879:DOATO>2.0.CO;2

Naylor J, Askelson MA, Gilmore MS (2012) Influence of low-level thermodynamic structure on the downdraft properties of simulated supercells. *Monthly Weather Review* **140**, 2575–2589. doi:10.1175/MWR-D-11-00200.1

Proctor FH (1989) Numerical simulations of an isolated microburst. Part II: sensitivity experiments. *Journal of the Atmospheric Sciences* **46**, 2143–2165. doi:10.1175/1520-0469(1989)046<2143:NSOAIM>2.0.CO;2

Rasmussen EN, Blanchard DO (1998) A baseline climatology of sounding-derived supercell and tornado forecast parameters. *Weather and Forecasting* **13**, 1148–1164. doi:10.1175/1520-0434(1998)013<1148:ABCOSD>2.0.CO;2

Saha S, Moorthi S, Pan H-L, Wu X, Wang J, Nadiga S, Tripp P, Kistler R, Woollen J, Behringer D , *et al.* (2010) The NCEP climate forecast system reanalysis. *Bulletin of the American Meteorological Society* **91**, 1015–1057. doi:10.1175/2010BAMS3001.1

Srivastava RC (1985) A simple model of evaporatively driven downdraft: application to microburst downdraft. *Journal of the Atmospheric Sciences* **42**, 1004–1023. doi:10.1175/1520-0469(1985)042<1004:ASMOED>2.0.CO;2

Srivastava RC (1987) A model of intense downdrafts driven by melting and evaporation of precipitation. *Journal of the Atmospheric Sciences* **44**, 1752–1774. doi:10.1175/1520-0469(1987)044<1752:AMOIDD>2.0.CO;2

Surveys and Investigation Staff (1981) A report to the committee on appropriations US House of Representatives on wildfire on Merritt Island. December 1981. (Washington, DC, USA). Available at https://www.wildfirelessons.net/HigherLogic/System/DownloadDocumentFile.ashx?DocumentFileKey=de70dc82-1760-487f-b1d4-05a8d11293cc&forceDialog=0 [Verified 26 July 2017].

Wakimoto RM (1985) Forecasting dry microburst activity over the High Plains. *Monthly Weather Review* **113**, 1131–1143. doi:10.1175/1520-0493(1985)113<1131:FDMAOT>2.0.CO;2